Autophagy promotes resistance to photodynamic therapy-induced apoptosis selectively in colorectal cancer stem-like cells

Ming-Feng Wei,[1] Min-Wei Chen,[2] Ke-Cheng Chen,[1,3] Pei-Jen Lou,[4] Susan Yun-Fan Lin,[1] Shih-Chieh Hung,[5] Michael Hsiao,[6] Cheng-Jung Yao,[7] and Ming-Jium Shieh[1,2,*]

[1]Institute of Biomedical Engineering; National Taiwan University; Taipei, Taiwan; [2]Department of Oncology; National Taiwan University Hospital; Taipei, Taiwan; [3]Department of Surgery; National Taiwan University Hospital; Taipei, Taiwan; [4]Department of Otolaryngology; National Taiwan University Hospital; Taipei, Taiwan; [5]Institute of Clinical Medicine; National Yang-Ming University; Taipei, Taiwan; [6]Genomics Research Center; Academia Sinica; Taipei, Taiwan; [7]Gastroenterology; Taipei Medical University-Municipal Wan Fang Hospital; Taipei, Taiwan

Recent studies have indicated that cancer stem-like cells (CSCs) exhibit a high resistance to current therapeutic strategies, including photodynamic therapy (PDT), leading to the recurrence and progression of colorectal cancer (CRC). In cancer, autophagy acts as both a tumor suppressor and a tumor promoter. However, the role of autophagy in the resistance of CSCs to PDT has not been reported. In this study, CSCs were isolated from colorectal cancer cells using PROM1/CD133 (prominin 1) expression, which is a surface marker commonly found on stem cells of various tissues. We demonstrated that PpIX-mediated PDT induced the formation of autophagosomes in PROM1/CD133+ cells, accompanied by the upregulation of autophagy-related proteins ATG3, ATG5, ATG7, and ATG12. The inhibition of PDT-induced autophagy by pharmacological inhibitors and silencing of the *ATG5* gene substantially triggered apoptosis of PROM1/CD133+ cells and decreased the ability of colonosphere formation in vitro and tumorigenicity in vivo. In conclusion, our results revealed a protective role played by autophagy against PDT in CSCs and indicated that targeting autophagy could be used to elevate the PDT sensitivity of CSCs. These findings would aid in the development of novel therapeutic approaches for CSC treatment.

Introduction

Colorectal cancer (CRC) is the fourth most common cause of cancer-related mortality worldwide, with more than 1.2 million new cases and 600,000 deaths per year.[1] The relative survival rate of patients with unresectable metastatic lesions drops to only 5%.[2] In addition to surgery, radiation therapy, and chemotherapy, photodynamic therapy (PDT) is regarded as another anticancer modality for the treatment of advanced colorectal cancer. PDT is a promising therapeutic approach for malignant and premalignant tumors and other diseases.[3,4] With this technique, a photosensitizer is irradiated and excited by light of a specific wavelength and then transfers this energy to oxygen to cause reactive oxygen species (ROS) formation. Subcellular damage subsequently occurs at the site of photosensitizer accumulation, which further drives either apoptosis or necrosis.[5-8] Because PDT causes essentially no effect on connective tissues, the anatomical integrity of hollow organs such as the colon can be preserved in patients undergoing PDT. However, numerous studies have indicated that several

resistance mechanisms cause a reduction in the efficacy of PDT on cancer cells.[9-13] Therefore, to improve the therapeutic outcome of PDT in colorectal cancer, mechanisms of primary resistance to PDT must be clarified.

Recently, increasing evidence has suggested that a small subpopulation of cancer cells may play a resistant role during treatment, leading to tumor recurrence and progression. Accordingly, these malignant cells responsible for tumor development and sustained tumor growth have been termed "cancer stem-like cells" (CSCs).[14] CSCs are thought to possess stem cell-like properties such as self-renewal and differentiation. The existence of CSCs has implications for novel cancer therapeutics, as the effective eradication of CSCs will likely be essential for successful cancer treatment.[15] Currently, CSCs are identified by their expression of specific surface markers; recent investigations have identified CSCs isolated from colorectal tumors with PROM1/CD133, a surface marker commonly found on the stem cells of various tissues.[16,17] Many studies propose that CSCs are resistant to chemotherapy and radiotherapy.[18-21] It has also been reported that side population (SP) stem cell-like cancer cells, which are considered CSCs, are resistant to PDT compared with non-SP cells.[22] However, a more detailed cellular mechanism underlying the resistance to PDT in CSCs remains poorly understood.

Autophagy is a dynamic process that involves the transport of cellular organelles and proteins through a lysosomal degradation pathway, and has been shown to play a variety of important roles related to cell survival, differentiation, and development.[23,24] Autophagy is regulated by a series of autophagy-related genes (*ATG*) that mediate the formation of the autophagosome and the activity of the PI3K-MTOR (phosphoinositide 3-kinase-mechanistic target of rapamycin) pathway controls autophagic flux.[25,26] Recent studies have shown that autophagy is involved in cancer development and progression and is activated by anticancer therapy.[27-29] It has been reported that autophagy can be induced by PDT.[30] Although the role played by autophagy in cell survival and cell death is still unclear, accumulating data show that an increase in autophagy levels can protect cancer cells against various apoptotic stimuli.[31-34] In addition, further studies are needed to determine the function of autophagy in CSCs and if autophagy can be induced by PDT in CSCs.

In this study, we examined the induction of autophagy by PDT and its role in colorectal PROM1/CD133+ CSCs. We found that CSC-enriched colorectal cancer cells would have more autophagosome formation than non-CSC-enriched cancer cells as shown by higher expression of autophagy-related proteins in CSC-enriched colorectal cancer cells. We also found that the maintenance, self-renewal, and resistance of CSCs after PDT treatment are dependent on autophagy. Inhibition of autophagy, both by an autophagy inhibitor and silencing of *ATGs,* sensitized the CSCs to PDT in vitro and in vivo. These results suggest that autophagy inhibition might abrogate CSC's resistance to PDT. Therefore, PDT combining autophagy inhibition might be a more efficient therapeutic approach for CSC treatment.
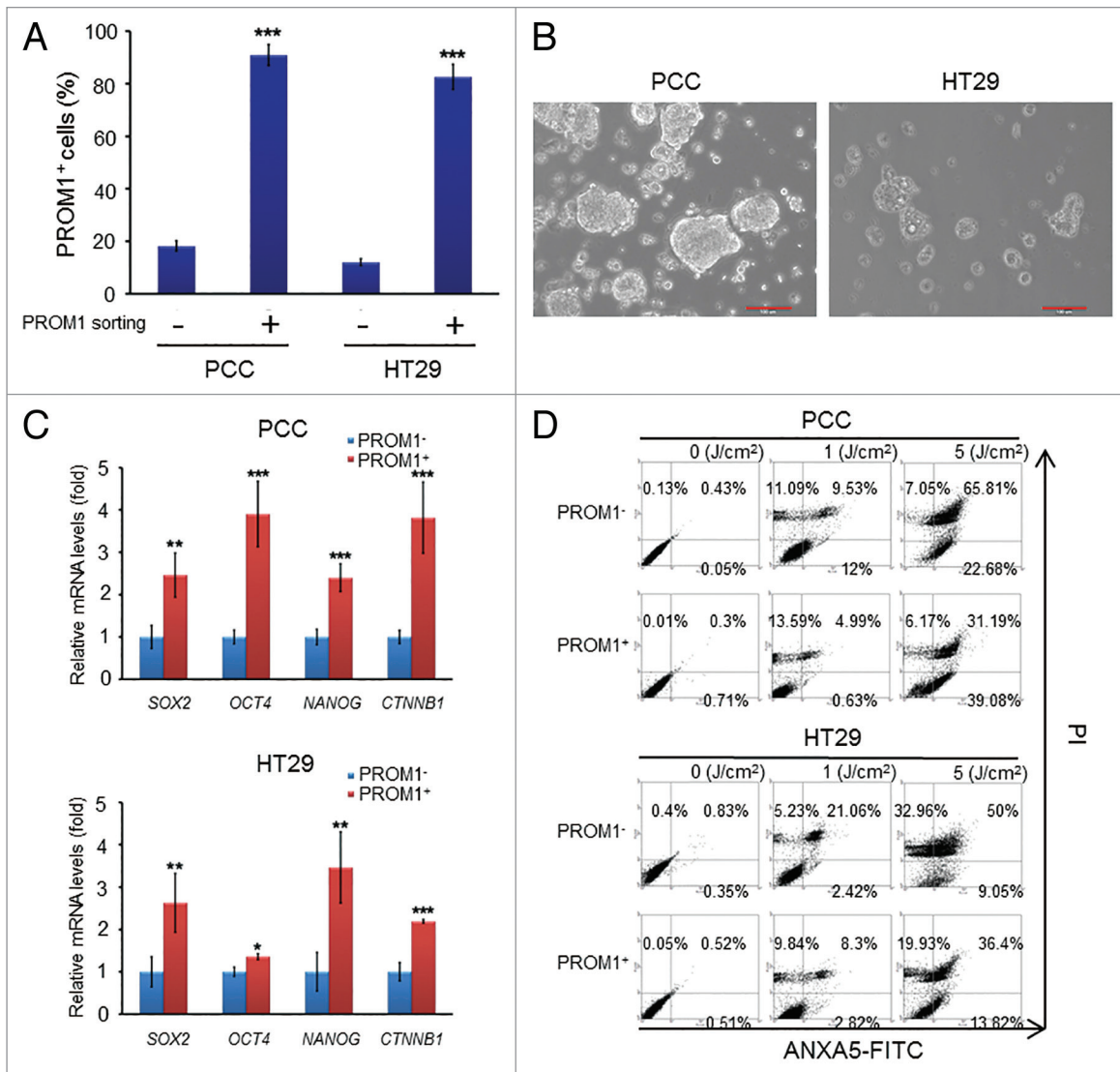
Results

PROM1/CD133+ cells of colorectal cancer exhibit the characteristics of CSCs and resistance to PDT

It has been shown that PROM1/CD133+ subpopulations in colorectal cancer cells exhibit colorectal cancer stem cell properties.[16] To verify whether PROM1/CD133+ cells exhibit cancer stem cell properties, we separated PROM1/CD133+ and PROM1/CD133– subpopulations from primary colorectal tumor (PCC) and HT29 colorectal cancer cells. After cell sorting, 80% of the cell population was PROM1/CD133+ (**Fig. 1A**). To analyze the stemness-associated properties of the isolated PROM1/CD133+ cells, sphere forming, stemness gene expression and drug sensitization assays were performed. The isolated PROM1/CD133+ cells could form clonal nonadherent 3D spheres (**Fig. 1B**) and were more resistant to conventional chemotherapy (**Fig. S1**). In contrast, fewer PROM1/CD133– cells could form spheres than the PROM1/CD133+ cells. The expression of stemness-related genes, such as *SOX2*, *POU5F1/ OCT4*, and *NANOG*, was higher in PROM1/CD133+ cells than PROM1/CD133– cells (**Fig. 1C**).

Previous studies demonstrate that SP cells are more resistant to PDT than non-SP cells.[22] To verify whether PROM1/CD133+ cells from PCC and HT29 cells exhibit similar resistance, PpIX-mediated PDT was utilized. PpIX is a naturally occurring photosensitizer used to detect and treat cancer. Cells were treated with PpIX in medium and then subjected to laser irradiation, which has a specific wavelength of 633 nm, at various doses. Cell survival after PDT treatment was analyzed by ANXA5/annexin V-FITC-PI staining. PpIX-mediated PDT caused significantly less PROM1/CD133+ cell death compared with PROM1/CD133– cells at the same irradiation dose (**Fig. 1D**; **Fig. S2**). These data showed that PROM1/CD133+ colorectal cancer cells were less sensitive to PDT than PROM1/CD133– cells. In addition, after PDT treatment, clonogenic survival fractions in both PCC and HT29 cell lines were reduced (**Fig. S3**) and suggested PDT resistance effect in PROM1/CD133+ cells. WST-1 assays also have similar results (**Fig. S4**). These data confirmed that PROM1/CD133+ cells have CSC-like properties, such as generation of spheres, high expression of stemness-associated genes, and high resistance to chemotherapeutic drugs and PDT.

PDT induces autophagy in PROM1/CD133+ cells

Numerous investigations indicated that autophagy, which is frequently activated in response to chemotherapy or radiotherapy, may contribute to resistance of different carcinoma cells.[35-40] Recent findings have also shown that autophagy could be induced in response to PDT in cancers cell lines and acts as a defense mechanism against PDT-mediated cellular damage.[41] To elucidate the extent of autophagy after treatment with PpIX-mediated PDT in colorectal CSCs, we analyzed the accumulation of LC3-II, the lipidated form of LC3 associated with the autophagosomal membrane, in the isolated PROM1/CD133+ cells. The amount of LC3-II reflects the number of autophagosomes. The accumulation of LC3-II markedly increased in PROM1/CD133+ cells at 24 h post-PDT with a laser irradiation dose of 1.3 J/cm^2 (~IC$_{50}$ of PROM1/CD133– cells) (**Fig. 2A**).

Figure 1. PROM1/CD133^{+} cells of colorectal cancer exhibit the characteristics of CSCs and resistance to PDT. (**A**) The PROM1/CD133^{+} cells were isolated from PCC or HT29 by FACS sorting. The percentage of PROM1/CD133^{+} cells was determined by FACS assay. (**B**) The morphology of PROM1/CD133^{+} cells was observed 10 d after FACS sorting. The PROM1/CD133^{+} cells formed floating tumorspheres under stem-cell conditions in the presence of EGF and FGF2. Scale bar: 100 μm. (**C**) Total RNA was isolated from PROM1/CD133^{−} and PROM1/CD133^{+} cells from PCC and HT29 cells and then analyzed by qPCR for *SOX2*, *OCT4*, *NANOG*, and *CTNNB1*. (**D**) Following PpIX-mediated PDT at various light doses, PROM1/CD133^{+} and PROM1/CD133^{−} cells viability was analyzed by ANXA5-FITC-PtdIns staining at 24 h after PDT. These results are expressed as the mean ± SE of 3 different experiments. *$P < 0.05$; **$P < 0.01$; ***$P < 0.001$.

The levels of autophagy were also observed by the formation of autophagosomes, as visualized using an anti-LC3 antibody. The number of LC3 puncta notably increased in PROM1/CD133^{+} PCC or HT29 cells after treatment with PDT (1.3 J/cm²) (**Fig. 2B**). In addition, acridine orange (AO) staining, a lysosomotropic dye that enters acidic compartments and emits bright red fluorescence, was used to assess the levels of autophagy by flow cytometry.[42] PROM1/CD133^{+} cells treated with PDT (1.3 J/cm²) displayed intense AO fluorescence (**Fig. 2C**). These data demonstrated that PDT-stimulated autophagy is robustly active in PROM1/CD133^{+} cells.

PDT-induced autophagy protects PROM1/CD133^{+} cells from PDT-induced cell death

To understand whether the autophagy induced by PDT has a role in PROM1/CD133^{+} cell escape from PDT treatment, the autophagy inhibitors chloroquine (CQ) and 3-methyladenine (3-MA) were used to examine the cytotoxicity of PCC and HT-29 cells treated with PDT. To determine the concentrations that effectively suppress autophagy but have only minimal cytotoxicity, CQ and 3-MA were analyzed by WST-1 assays and western blotting (**Fig. S5 and S6**). The appropriate concentrations were found to be 10 μM and 5 mM for CQ and 3-MA, respectively. Treatment of PROM1/CD133^{+} PCCs with either CQ or 3-MA significantly increased cytotoxicity in the PROM1/CD133^{+} cells treated with PDT compared with cells that did not receive CQ or 3-MA (**Fig. 3A**). Similar results
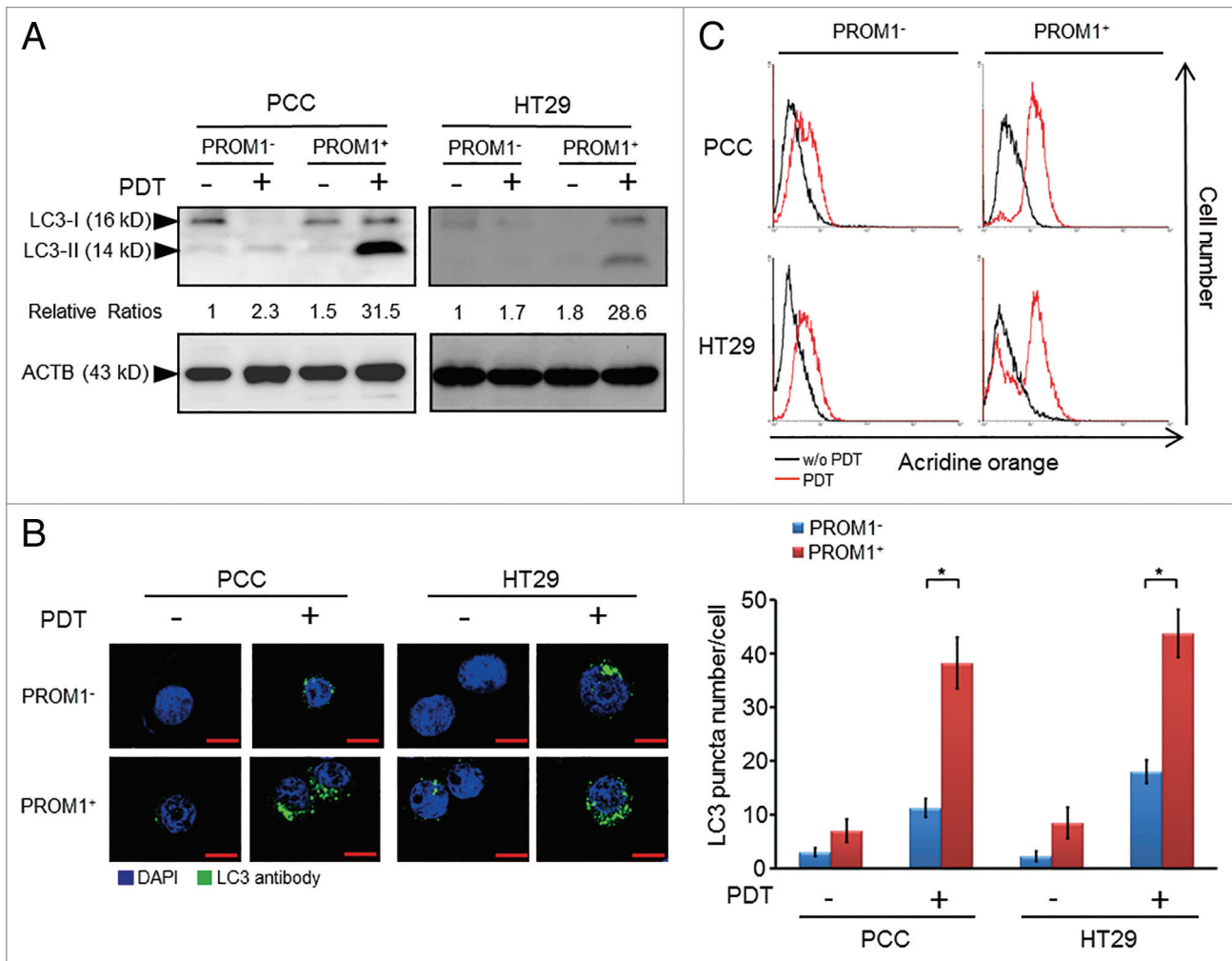
Figure 2. PpIX-mediated PDT leads to an increased level of autophagy in PROM1/CD133⁺ cells. (**A**) PROM1/CD133⁻ and PROM1/CD133⁺ cells were treated with PDT (1.3 J/cm²). After 24 h, total cell lysates were analyzed by western blot. The band intensities on films were analyzed by ImageJ software. The relative amounts of LC3-II were quantified as ratios to ACTB, indicated underneath each gel. The relative ratio of LC3-II in PROM1/CD133⁻ cells without PDT treatment is arbitrarily presented as 1. (**B**) Cells were labeled with anti-LC3 primary antibody and DyLight 488 conjugated secondary antibody at 24 h after PDT (1.3 J/cm²). LC3 puncta were observed by immunofluorescence using confocal microscopy. Nuclei were counterstained with DAPI. Scale bar: 10 μm. The number of LC3 puncta was counted using 20 cells for each condition. (**C**) Flow cytometric analysis of AO staining for cells at 24 h post PDT treatment (1.3 J/cm²). These results are expressed as the mean ± SE of 3 different experiments. *$P < 0.05$.

were observed in PROM1/CD133⁺ HT29 cells. In PROM1/CD133⁻ cells, no differences were observed in the cytotoxicity for cells treated with PDT in the presence or absence of CQ or 3-MA.

The ability to form spheres in nonadherent culture is one of the characteristics of CSCs. Descriptions of sphere-forming cells play an important role in understanding the maintenance of tumor growth and the ability of cancers to develop resistance to conventional therapy. To examine whether autophagy has a role in the ability of self-renewing sphere-forming cells to resist PDT, the sensitivity of colonosphere-forming cells to PDT alone or in combination with autophagy inhibitors was assessed. Spheres containing more than 20 cells were scored, and the PDT irradiation dose of 1.3 J/cm² was applied. We found that the number of colonospheres was reduced when they had been treated with CQ and subjected to PDT (**Fig. 3B**). Consistently, inhibition of

autophagy with either CQ or 3-MA in PROM1/CD133⁺ cells significantly decreased the ability of PROM1/CD133⁺ cells to form colonospheres following PDT treatment. In addition, the size of the newly formed spheres was markedly smaller (sphere size is smaller than 50 μm) in the group treated with PDT (1.3 J/cm²) in combination with autophagy inhibitors than in the control group or the group treated with PDT alone (**Fig. 3C**). These data indicated that, in PROM1/CD133⁺ cells treated with PDT in combination with autophagy inhibitors, not only was the cytotoxicity increased, but sphere-forming capacity of colon CSCs was also affected. Collectively, these data showed that induction of autophagy by PDT treatment contributes to the ability of PROM1/CD133⁺ cells to proliferate and self-renew, which makes PROM1/CD133⁺ cells resistant to PDT.

Silencing of autophagy-related genes sensitized PROM1/CD133⁺ cells to PDT
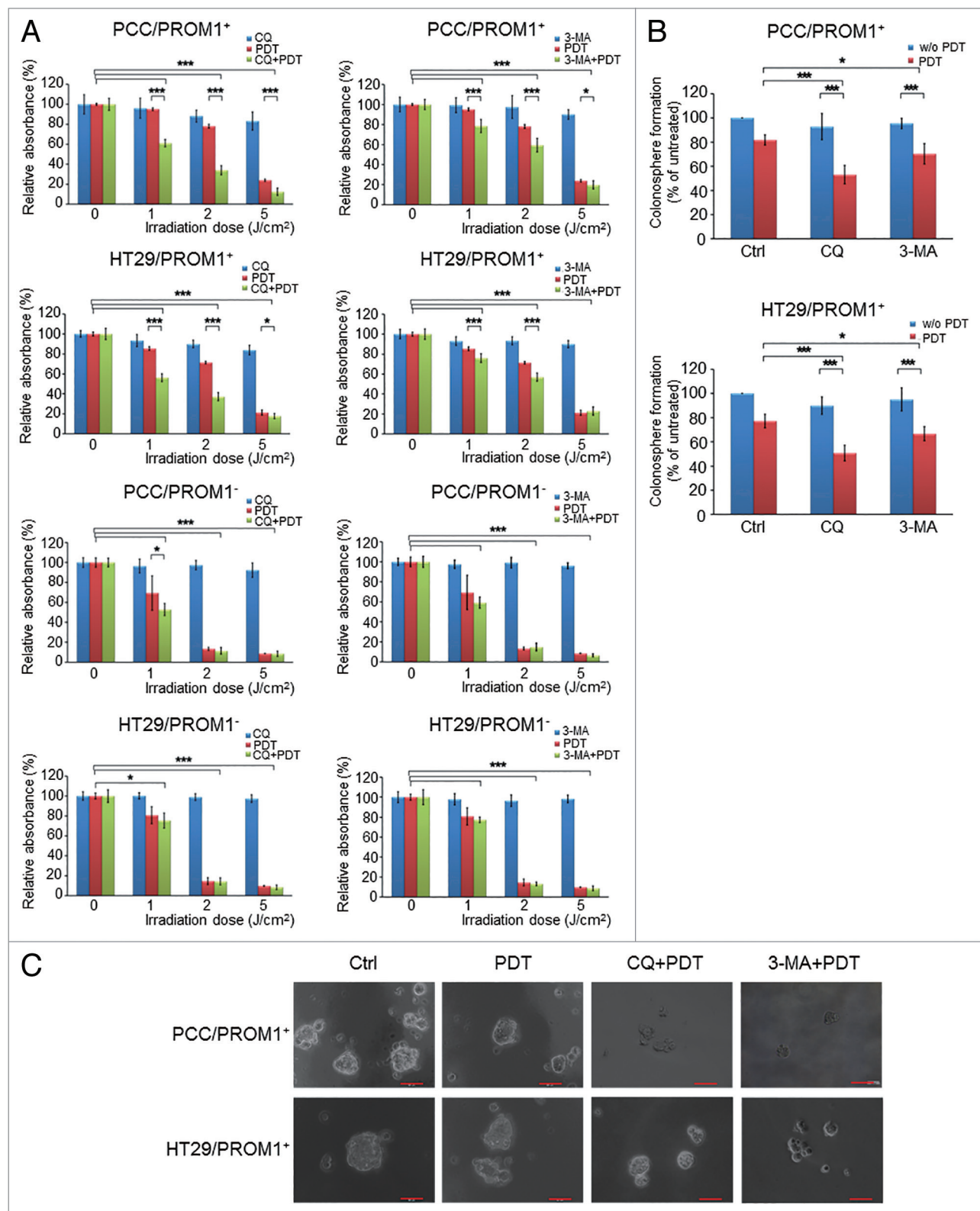
Figure 3. PpIX-mediated PDT combined with autophagy inhibitors enhanced the cytotoxic effect and blocked colonosphere formation in CSCs. (**A**) The PROM1/CD133⁺ and PROM1/CD133⁻ cells form PCCs and HT29 cells were treated with chloroquine (10 μM) or 3-MA (5 mM) for 24 h followed by PDT at various light doses. Cytotoxicity was measured using the WST-1 assay. (**B**) and (**C**) The disaggregated PROM1/CD133⁺ cells were plated at 100 cells/well in an ultra-low attachment plate and treated with PDT (1.3 J/cm²) in the presence of CQ or 3-MA. Colonospheres that contained at least 20 cells were counted in 8 different wells. Representative images show the sizes of the newly formed colonospheres after 7 d. Scale bar: 50 μm. The results are expressed as the mean ± SE of 3 different experiments. *$P < 0.05$; **$P < 0.01$; ***$P < 0.001$.

Autophagy-related proteins are involved in phagophore induction, cytoplasm engulfment, autophagic vesicle formation, and lysosomal fusion. The study demonstrated that PROM1/CD133+ cells express higher levels of the autophagy-related proteins LC3, ATG5, and ATG12, which are involved in autophagosome formation, than PROM1/CD133− cells after irradiation, and inhibition of autophagy preferentially sensitizes PROM1/CD133+ cells to irradiation and decreases their sphere-forming capacity.[43] To further understand the molecular machinery of autophagy induced by PDT, western blotting was performed. The PROM1/CD133+ cells treated with PDT (1.3 J/cm^2) expressed higher levels of the autophagy-related proteins, including ATG3, ATG5, ATG7, and ATG12, than PROM1/CD133− cells (**Fig. 4A**). This result indicated that PDT-induced ATG expression in PROM1/CD133+ cells may be responsible for the increase in the levels of autophagy after PDT.

To further elucidate whether ATG mediate PDT-induced autophagy and contribute to PDT resistance in PROM1/CD133+ cells, a knockdown experiment was performed. As chemical inhibitors of autophagy may lead to off-target effects, specific shRNAs of *ATG3* and *ATG5*, which are genes whose protein products are involved in 2 essential ubiquitin-like conjugation systems in autophagy, were used. Western blot analysis showed efficient knockdown of *ATG3* and *ATG5* in PROM1/CD133+ cells (**Fig. 4B**). We further examined the influence of sh*ATG3* and sh*ATG5* on PDT-induced LC3-II accumulation in PROM1/CD133+ cells (**Fig. S7**). LC3-II accumulation was markedly decreased in *ATG*-silenced PROM1/CD133+ cells after PDT.

Next, we examined the cytotoxicity of the *ATG*-silenced PROM1/CD133+ PCCs subjected to PDT. Silencing of *ATG3* or *ATG5* significantly increased the cytotoxicity of PDT in PROM1/CD133+ cells compared with the effect observed by scrambled shRNA in PROM1/CD133+ cells, and silencing of *ATG3* or *ATG5* without PDT treatment did not cause significant cell death (**Fig. 4C**). In PROM1/CD133− PCCs, no differences were observed in the cytotoxicity for cells treated with PDT either in the presence or absence of silencing of *ATG3* or *ATG5*. Similar results were observed in both the PROM1/CD133+ and PROM1/CD133− populations of HT29 cells. In addition, the ability of *ATG*-silenced PROM1/CD133+ PCCs to form colonospheres was also significantly reduced, resembling the results caused by the pharmacological inhibitors (**Fig. 4D and E**). The genetic silencing of *ATGs* remarkably improved the cytotoxicity of PDT and attenuated the stemness-associated properties of the PROM1/CD133+ cells. Together, these data further showed that after PDT treatment, PROM1/CD133+ cells not only expressed more ATGs but also activated higher levels of autophagy to lead to PDT resistance.
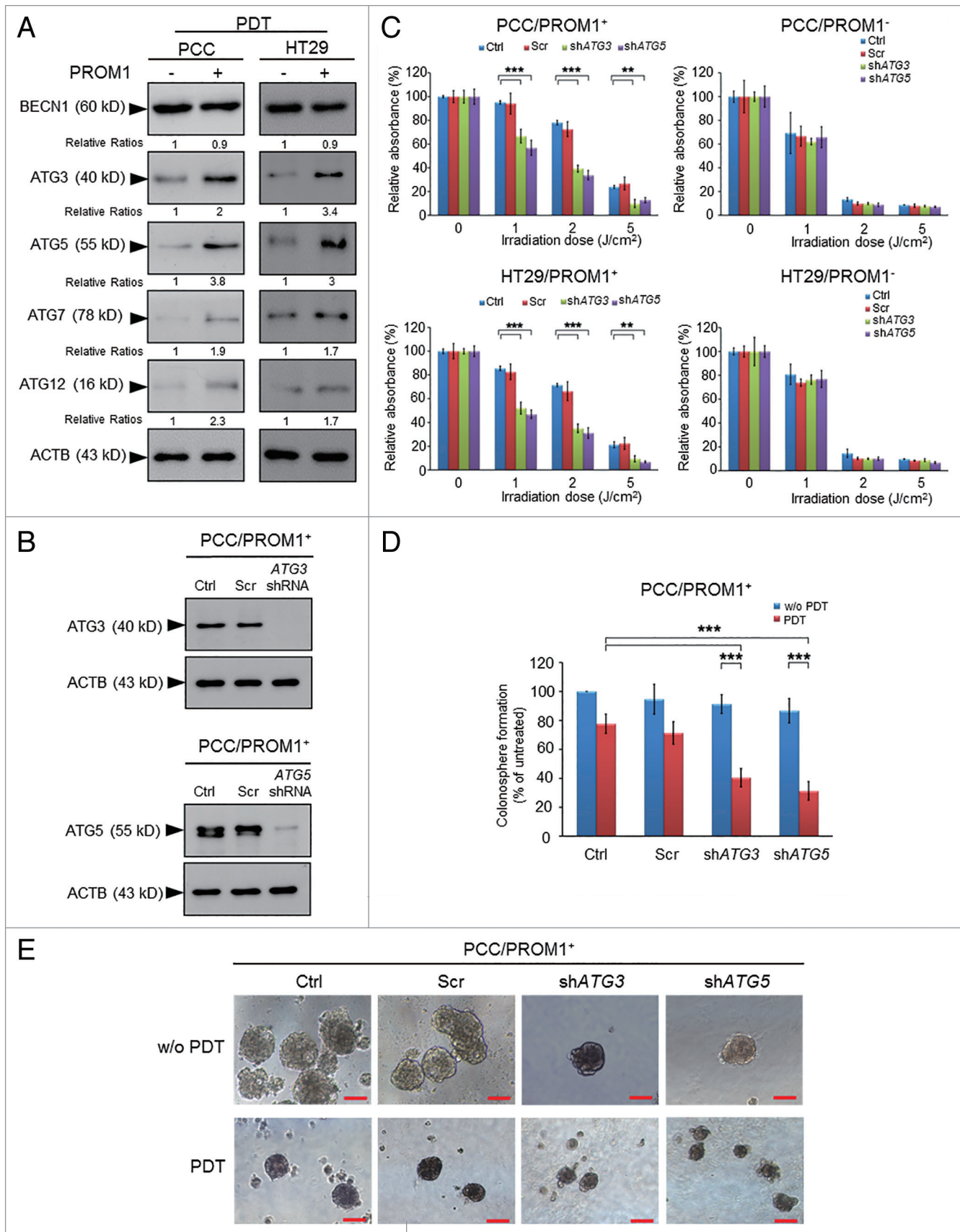
Inhibition of PDT-induced autophagy enhances the apoptotic effect of PDT in PROM1/CD133+ cells

Many previous reports have indicated that autophagy can perform 2 seemingly opposite roles, prosurvival or prodeath, and it can cause resistance to apoptosis when induced by anticancer therapy.[44] It is well known that PDT can induce cell death through apoptosis or necrosis both in vitro and in vivo.[45] Here, we investigated whether inhibition of autophagy enhances apoptotic effects in PROM1/CD133+ cells. Both chemical inhibition of autophagy and depletion of *ATG5* in PROM1/CD133+ PCCs resulted in massive apoptosis following PDT detected by a TUNEL assay compared with the control group or the group treated with PDT alone (**Fig. 5A**). In addition, CASP3/caspase-3 activity and ANXA5-FITC-PI staining were performed to measure the apoptosis level in each treatment group. As presented in **Figure 5B and C**, both chemical inhibition of autophagy and depletion of *ATG5* enhanced apoptosis after PDT treatment, as shown by a significant elevation of CASP3 activity and an increase in the percentage of ANXA5-positive cells. In contrast, without PDT treatment, CQ-treated or *ATG5*-silenced PROM1/CD133+ cells showed only slight increases in apoptosis. These results indicated that autophagy plays a protective role for PROM1/CD133+ cells by modulating apoptosis in response to PDT. Therefore, autophagy acts as an antiapoptotic mechanism for CSCs under stress induced by PDT.

**Blocking autophagy enhances the antitumorigenicity of PDT in a xenograft model**

To assess the PDT resistance effect of autophagy in PROM1/CD133+ cells, in vivo tumorigenicity after PDT pretreatment in vitro was assayed. Specifically, the in vivo tumorigenicity of PROM1/CD133+ cells pretreated with CQ or sh*ATG5* following PDT treatment (1.3 J/cm^2) in vitro in NOD/SCID mice were analyzed. For the positive control, mice were inoculated with 1×10^3 PROM1/CD133+ cells, and 87.5% (7/8) of the mice in that group developed tumors. For the experimental group, mice were inoculated with 1×10^3 viable PROM1/CD133+ cells that were subjected to PDT, and 75% (6/8) of the mice in that group developed tumors. This result indicates PDT did not suppress in vivo tumorigenicity. The incidence of tumor formation was lower when CQ-treated or *ATG5*-silenced PROM1/CD133+ cells subjected to PDT were injected into NOD/SCID mice (both are 2/6) than when CQ-treated or *ATG5*-silenced PROM1/CD133+ cells that were not subjected to PDT were injected into NOD/SCID mice (**Table 1**). As expected, tumor volume was lowest with CQ-treated or *ATG5*-silenced PROM1/

Figure 4 (See opposite page). Genetic silencing of autophagy enhances the cytotoxic effect of PpIX-mediated PDT in the CSCs. (**A**) The total extracts of PROM1/CD133− and PROM1/CD133+ cells were harvested at 24 h post-PDT (1.3 J/cm^2). The levels of ACTB and autophagy-related proteins, including ATG3, ATG5, ATG7, ATG12, and BECN1, were assessed by western blot analysis. The band intensities on films were analyzed by ImageJ software. The relative amounts of each protein were quantified as ratios to ACTB, indicated underneath each gel. The relative ratio of each protein in PROM1/CD133− cells is arbitrarily presented as 1. (**B**) The PROM1/CD133+ PCCs were infected with *pGIPZ* lentivirus (scrambled), *ATG3* or *ATG5* shRNA lentivirus. The protein expression of ATG3 and ATG5 was examined by western blot analysis. (**C**) The PROM1/CD133+ PCCs and PROM1/CD133+ HT29 cells that expressed specific shRNA were treated with PDT at various light doses. The cytotoxicity was then measured using the WST-1 assay. (**D and E**) The disaggregated PROM1/CD133+ PCCs that expressed specific shRNA were plated at 100 cells/well in an ultra-low attachment plate and treated with PDT (1.3 J/cm^2). The number and size of the colonospheres were assessed as described for **Figure 3**. Scale bar: 50 μm. The results are expressed as the mean ± SE of 3 different experiments. *$P < 0.05$; **$P < 0.01$; ***$P < 0.001$.

Figure 4. For figure legend, see page 1184.
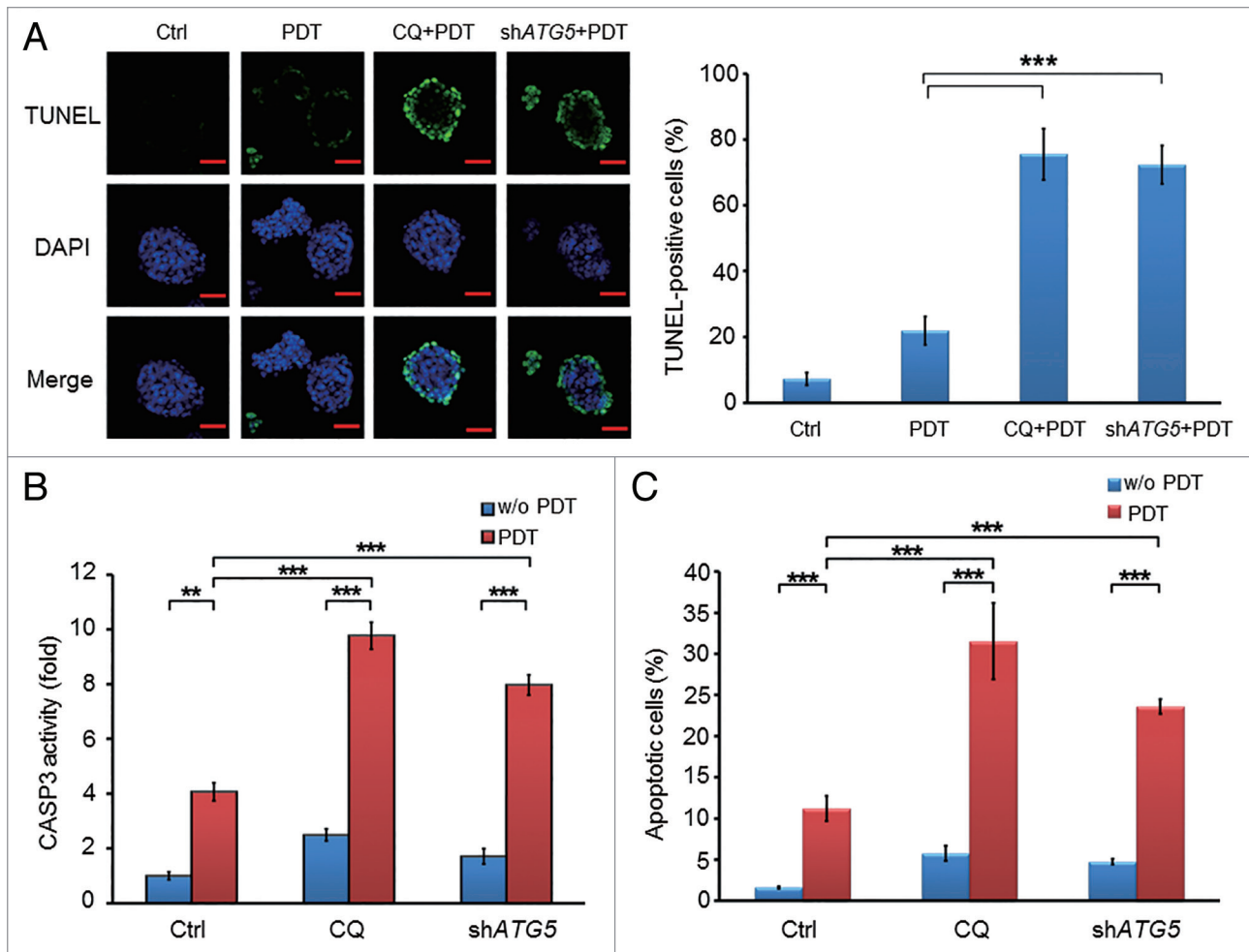
Figure 5. Inhibition of autophagy by chloroquine or *ATG5* shRNA enhanced the apoptotic effect of PDT in CSCs. (**A**) Apoptotic cells of PROM1/CD133⁺ PCCs were visualized by TUNEL assay at 24 h post-PDT (1.3 J/cm²). Nuclei were specifically labeled using DAPI staining. Scale bar: 50 μm. The percentage of TUNEL-positive cells was scored per 100 cells. (**B**) Whole cell lysates of PROM1/CD133⁺ PCCs were collected at 24 h post-PDT (1.3 J/cm²) and measured by CaspACE™ Assay System for CASP3 activities. (**C**) The percentage of apoptotic cells of PROM1/CD133⁺ PCCs was monitored by ANXA5-FITC-PtdIns staining and flow cytometry at 24 h post-PDT (1.3 J/cm²), and apoptotic ratio was calculated by plotting ANXA5-FITC-positive cell number against total cell number. These results are expressed as the mean ± SE of 3 different experiments. *$P < 0.05$; **$P < 0.01$; ***$P < 0.001$.

Table 1. Tumor-initiating potential of PROM1/CD133⁺ PCCs in each treatment group

Cells injected	1 × 10³
Control	7/8
PDT	6/8
CQ	5/6
CQ+PDT	2/6
sh*ATG5*	6/6
sh*ATG5*+PDT	2/6

A total of 1 × 10³ viable PROM1/CD133⁺ PCCs, pretreated with PDT, CQ, sh*ATG5* lentivirus, either alone or in the indicated combinations, were implanted subcutaneously into both flanks of NOD/SCID mice. Tumor-initiating potential in each treatment group was observed.

CD133⁺ cells following PDT; however, CQ-treated or *ATG5*-silenced PROM1/CD133⁺ cells without PDT did not affect tumor growth (**Fig. 6A**). These results were consistent with the findings of the in vitro assay of self-renewal potential (**Fig. 3**; **Fig. 4**).

Subsequently, these tumor burdens were measured. The results showed that the tumors in CQ-treated and *ATG5*-silenced groups were significantly distributed in lower tumor volume ranges with PDT compared with without PDT (**Fig. 6B**). Taken together, our results suggested that PDT combined with autophagy inhibition was effective in reducing the tumorigenic potential of PROM1/CD133⁺ cells. These findings not only further verified that PDT-induced autophagy is responsible for PDT resistance in PROM1/CD133⁺ cells but also opened a new avenue for potentially treating CSC through combination therapy of PDT and autophagy inhibition.
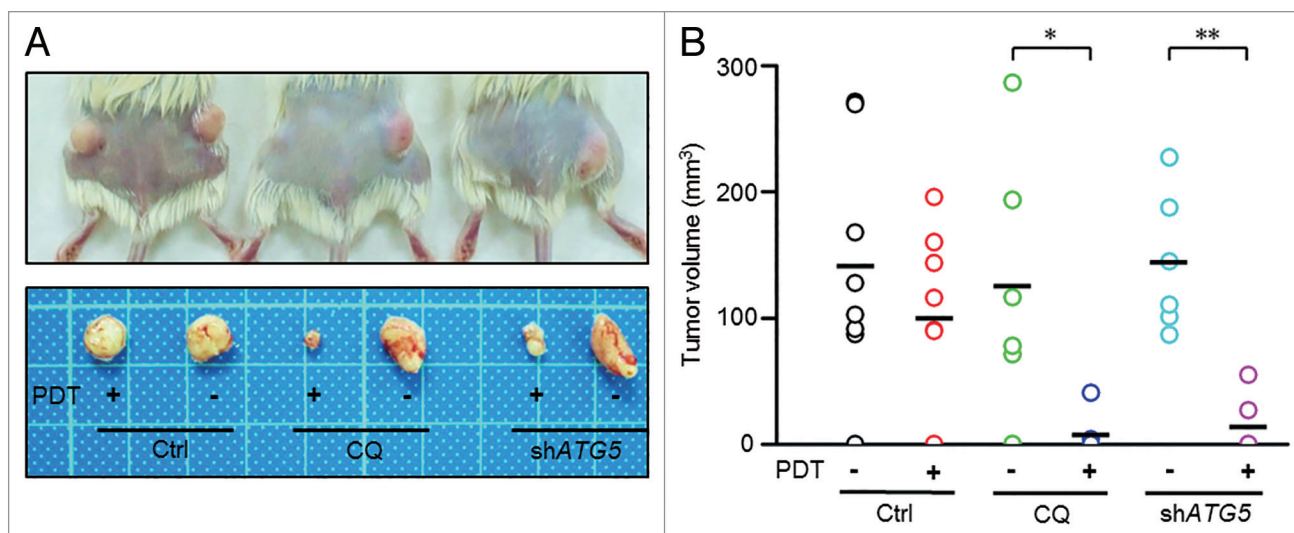
Figure 6. Inhibition of autophagy enhanced the antitumorigenicity of PDT in a xenograft model. (**A**) A total of 1×10^3 viable PROM1/CD133$^+$ PCCs, pretreated with CQ (10 μM), *ATG5* shRNA lentivirus, or PDT (1.3 J/cm^2), either alone or in the indicated combinations, were implanted subcutaneously into both flanks of NOD/SCID mice. Representative pictures of each treatment group. Mice were sacrificed 12 wk after implantation. (**B**) Tumor sizes were measured at the end of the experiment. Data are presented as dot plots, and the short black lines indicate mean tumor size. Tumor volume was calculated as (L * W^2)/2, where L is the length and W is the width of the tumor. The tumors in CQ-treated and *ATG5*-silenced groups were significantly distributed in lower tumor volume ranges with PDT compared with without PDT. *$P < 0.05$; **$P < 0.01$.

Discussion

Currently, all existing therapeutic approaches for CRC have high risks of recurrence. The hypothesis of cancer stem-like cells (CSCs) identifies the possibility that a small subpopulation of cancer cells may result in therapeutic failure for cancer patients.[14] Over the years, CSCs have been specifically shown to cause tumor relapse and therapeutic resistance;[46] therefore, it is important to find the mechanisms of resistance to anticancer therapies in CSCs.

So far, CSCs are thought to demonstrate resistance to chemotherapeutic agents and radiation mainly due to their expressions of multidrug transporter family genes and DNA damage response genes.[18-21] Numerous studies have indicated that ATP-binding cassette (ABC) transporters can affect PDT efficacy by pumping out photosensitizers.[11,47] However, from our unpublished data, we have observed that PROM1/CD133$^+$ cells, which are considered CSCs for CRC, can accumulate more PpIX in comparison to PROM1/CD133$^-$ cells. This result implies that there must be other mechanisms of resistance to PDT in CSCs. PDT can induce cell death by generating many ROS which are believed to be key regulators of autophagy in cancer cells.[7,8,48-50] Autophagy is an important mechanism mediating the resistance of cancer cells to various therapeutic strategies.[29,35-40] Therefore, we inferred that autophagy might be a major cause of PDT-resistance in CSCs.

In a previous study, the level of LC3-II and autophagosome synthesis are higher in mammospheres than in adherent cells under both basal and starvation conditions.[51] In addition, PROM1/CD133$^+$ cells show higher activity of autophagy by forming more autophagic puncta and causing more accumulation of LC3-II compared with PROM1/CD133$^-$ cells under low-nutrient conditions.[52] Similarly, we had also observed increased autophagic characteristics in PROM1/CD133$^+$ cells in response to PpIX-mediated PDT. This finding implied that PDT could result in high levels of autophagy activation in CSCs. Simultaneously, we found that PROM1/CD133$^+$ cells with the stimulus of PDT expressed higher levels of the autophagy-related proteins, ATG3, ATG5, and ATG7. The increased expression of these autophagy-related proteins may enhance the levels of autophagy in PDT-treated CSCs. Furthermore, we demonstrated that autophagy inhibition with pharmacological inhibitors or silencing of *ATG3* and *ATG5* could significantly enhance the sensitivity of PROM1/CD133$^+$ cells to PpIX-mediated PDT by a cytotoxicity and colonosphere formation assay. However, there were no differences in the cytotoxicity of PROM1/CD133$^-$ cells undergoing PDT treatments either in the presence or absence of CQ. This result suggested that autophagy most likely plays no role in influencing PROM1/CD133$^-$ cells' response to PDT. Our result is consistent with a previous report demonstrating that autophagy exerts a protective role against chemotherapy and radiotherapy in CSCs.[43,53] These findings all highlighted the fact that autophagy must contribute to the resistance of CSCs to PDT.

It is well known that PDT-generated ROS could concurrently induce both autophagy and apoptosis pathways in cancer cells.[54,55] Accumulating data propose that autophagy may antagonize apoptosis.[56-59] This evidence indicates that cancer cells could enhance autophagy to decrease apoptosis. On the other hand, inhibition of autophagic flux could accelerate the proapoptotic capacity of therapeutic modalities when treating CSCs.[60] Our study also consistently showed that PROM1/CD133$^+$ cells with autophagy inhibition were more susceptible to PDT-mediated apoptosis. To further elucidate the autophagy/
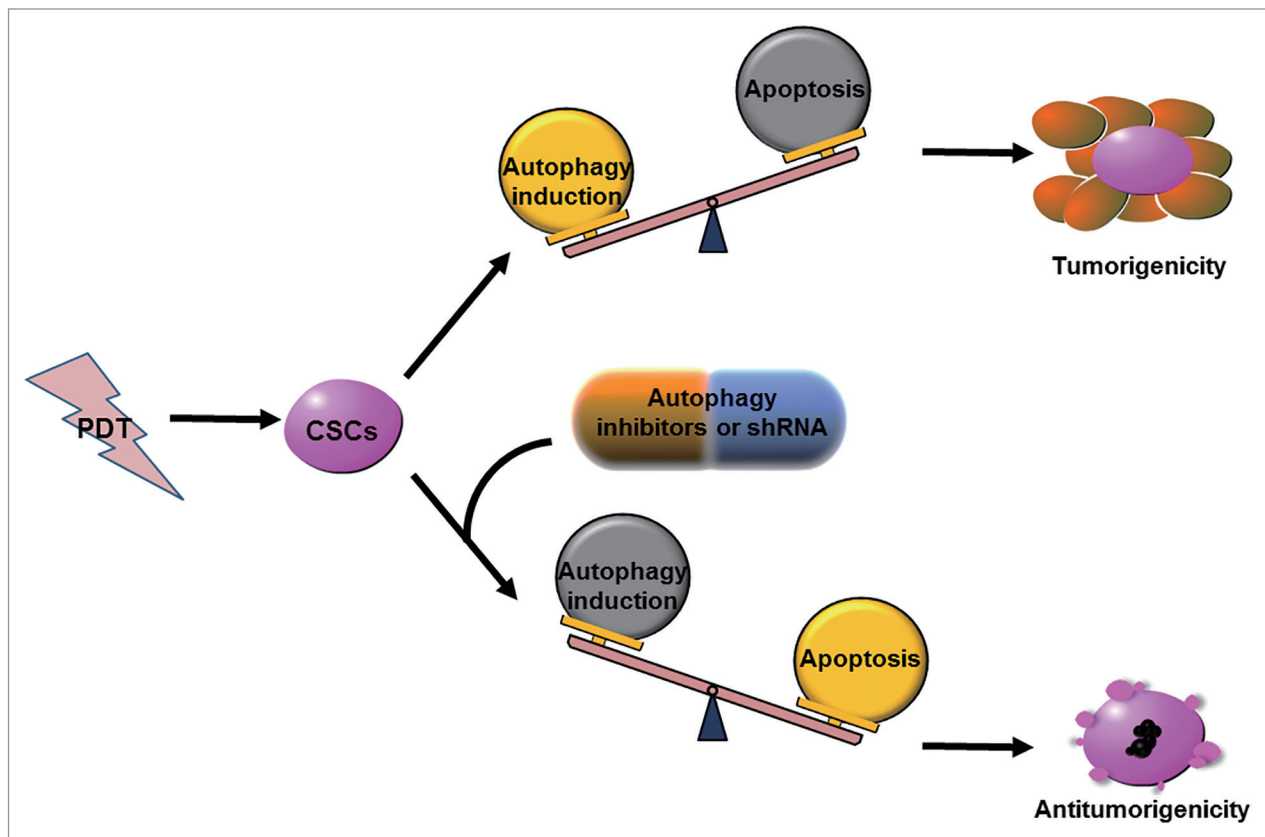
Figure 7. Model of antitumorigenicity ability of PDT combined with autophagy inhibition. Autophagy inhibition enhances CSC sensitivity to PDT and PDT-induced apoptosis, and dramatically reduces the tumorigenicity of CSCs under PDT treatment.

apoptosis interconnection, we discussed the roles played by ATG3 and ATG5. ATG3 and ATG5 are both essential regulatory components of autophagosome biogenesis.[61,62] A recent report shows that ATG3 degradation by CASP8 could lead to autophagy inactivation during receptor-triggered apoptosis.[63] Full-length ATG5 can participate in autophagy activation.[64,65] Under lethal stress, ATG5 is cleaved by CAPN/calpains, which triggers apoptosis via induction of MOMP (mitochondrial outer membrane permeabilization) or interaction with FADD (Fas [TNFRSF6]-associated via death domain).[64,66]

In both CSCs and malignant cells, autophagy could support tumor establishment and development.[67] Our present study clearly showed that the therapeutic strategy of PDT combined with autophagy inhibition could decrease tumorigenicity of PROM1/CD133+ cells in a xenograft model. Even the tumors that grew under combination treatment had significantly suppressed size. Altogether, it is very probable that autophagy inhibition played a key role in increasing apoptosis of PDT-treated PROM1/CD133+ cells and the consequent tumorigenicity reduction. However, when PROM1/CD133+ cells underwent PDT treatment without autophagy inhibition, there was no effect on tumorigenicity or tumor volume. This most likely indicates that CSC properties are affected by autophagy inhibition. Our data support a model in which autophagy inhibition enhances CSC sensitivity to PDT and PDT-induced apoptosis, and dramatically reduces the tumorigenicity of CSCs under PDT treatment (**Fig.** 7).

Overall, we demonstrated that PpIX-mediated PDT could significantly upregulate the levels of autophagy in PROM1/CD133+ cells. Suppressing autophagy could sensitize PROM1/CD133+ cells to apoptosis induced by PDT. In vitro spheroid formation and the in vivo tumorigenicity of PROM1/CD133+ cells were decreased after autophagy had been blocked. These results all imply that enhanced autophagy levels are related to the increase of resistance to PDT in CSCs. Therefore, our study not only revealed the possible mechanisms executed by autophagy in the resistance and tumorigenicity of CSCs after PDT but also provided a new therapeutic avenue for targeting autophagy in anti-CSC treatment with PDT.

Materials and Methods

Materials

PpIX was obtained from Sigma-Aldrich (P8293), dissolved in 100% dimethyl sulfoxide (DMSO; Sigma-Aldrich, D2650) to a concentration of 2 mg/ml. Chloroquine (Sigma-Aldrich, C6628) and 3-MA (Calbiochem, 189490) were dissolved in deionized water to create 1 mM and 100 mM stock solutions, respectively. The antibodies used included CD133/2-phycoerythrin (PE) (Miltenyi Biotec, 130-090-853) and isotype control IgG2b-PE (Miltenyi Biotec, 130-092-215).

PROM1/CD133+ cell isolation and culture

The colorectal cancer primary cultured cells (PCCs) were kindly provided by SC Hung (Institute of Clinical Medicine, School of Medicine, National Yang-Ming University, Taipei, Taiwan). After the PCCs and the HT29 cells (purchased from American Type Culture Collection, HTB-38 ™) were collected and stained with a CD133/2-PE antibody for 30 min, the PROM1/CD133+ cells were sorted using a FACSAria-I cell sorter (Becton Dickinson, CA, USA). The isolated PROM1/CD133+ cells were cultured under stem-cell conditions in serum-free DMEM/F12 medium (Gibco, 12500-062) supplemented with 20 ng/mL of human recombinant epidermal growth factor (EGF; PeproTech, AF-100-15), 10 ng/mL of FGF2 [fibroblast growth factor 2 (basic)] (bFGF; PeproTech, 100-18B), and 1% N-2 supplement (Gibco, 17502-048). The cells were cultured on ultra-low attachment plates (Corning Inc., 3471) for subsequent organization into spheres.[68]

Quantitative real-time PCR

Total RNA was isolated from PROM1/CD133− and PROM1/CD133+ cells from PCC and HT29 cells using the PureLink Micro-to-Midi Total RNA Purification system (Invitrogen, 12183-018). The reverse transcription reaction was performed using the SuperScript III First-Strand Synthesis system for RT-PCR (Invitrogen, 18080-051). Expression of *SOX2*, *OCT4*, *NANOG*, and CTNNB1/β-catenin was quantified using the ABI Prism 7900 real-time system (Applied Biosystems, Foster City, CA, USA) and their expression is normalized to *GAPDH*. All reactions were performed in triplicate. The following primers were used: *SOX2*: forward 5′-GTATCAGGAG TTGTCAAGGC-3′, reverse 5′-AGTCCTAGTC TTAAAGAGG-3′; *OCT4*: forward 5′-GCTCACCCTG GGCGTTCTC-3′, reverse 5′-GGCCGCAGCT TACACATGTTC-3′; *NANOG*: forward 5′-CCTCCAGCAG ATGCAAGAAC TC-3′, reverse 5′-CTTCAACCAC TGGTTTTTCT GCC-3′; *CTNNB1*: forward 5′-GAAACGGCTT TCAGTTGAGC-3′, reverse 5′-CTGGCCATAT CCACCAGAGT-3′; *GAPDH*: forward 5′-CATGAGAAGT ATGACAACAG CCT-3′, reverse 5′-AGTCCTTCCA CGATACCAAA GT-3′.

The identification of resistance to PDT

The PROM1/CD133+ and PROM1/CD133− cells were incubated in the dark for 3 h with 1 µg/mL PpIX. Then, the cells were washed twice with phosphate-buffered saline (PBS) and exposed to various doses (0 J/cm², 1 J/cm², and 5 J/cm²) of red light generated by a light-emitting diode (LED; 633 nm) for photodynamic treatment. The cells were then incubated in fresh medium under standard cell culture conditions for 24 h. PDT-induced cell death was analyzed using the Dead Cell Apoptosis Kit with ANXA5-FITC and PI (Molecular Probes®, V13242). The percentage of apoptotic cells was measured by flow cytometry. The results are expressed as the mean ± SE of 3 different experiments.

Immunofluorescence

The PROM1/CD133+ and PROM1/CD133− cells were plated on Tissue Culture Treated Glass Slide (BD Falcon, 354114) and subjected to PDT treatment (1.3 J/cm²). After 24 h, cells were washed with PBS and fixed with 3.7% paraformaldehyde for 8 min. Fixed cells were permeabilized with 0.1% Triton X-100 in PBS for 15 min, blocked with 3% BSA for 60 min, and incubated with anti-LC3 antibodies (1:200) (Cell Signaling Technology, 3868S) overnight. After washing with PBS, cells were incubated for 1 h with DyLight 488 conjugated secondary antibody (1:500) (BioLink Biotechnology, B0210). Nuclei were counterstained with DAPI (Biotium, 40043) for 5 min. Slides were mounted with a coverslip using Fluoro-Gel (Electron Microscopy Sciences, 17985-10). Cells were imaged using a confocal laser scanning microscope (TCS SP5, Leica Microsystems, Wetzlar, Germany), and the images were analyzed using a Leica Application Suite 2.02. DyLight 488 was excited using an argon laser (488 nm), and DAPI was excited using a diode laser (405 nm). The emission lights for DAPI and DyLight 488 were collected between 410 and 490 nm and between 495 and 540 nm, respectively.

Acridine orange staining

PROM1/CD133+ and PROM1/CD133− cells were treated with PDT (1.3 J/cm²) and stained with AO (1 µg/ml) (Sigma-Aldrich, A6014) at 37 °C for 30 min after 24 h post PDT treatment. After removing AO, the stained cells were immediately analyzed in the FL-3 channel using a FACSCalibur (Becton Dickinson, BD FACSCalibur™ system, CA, USA).

Cytotoxicity assay

Disaggregated PROM1/CD133+ and PROM1/CD133− cells were plated in 100 µl of medium at a concentration of 8,000 cells/well in 96-well plates and treated with PDT at various light doses in the presence or absence of CQ (10 µM), 3-MA (5 mM), sh*ATG3*, and sh*ATG5*. After 24 h, cell survival was measured using a Premixed WST-1 Cell Proliferation Reagent (Clontech, 630118), and the absorbance of each sample was measured at 450 nm against the background control using a multi-well plate reader. Cytotoxicity was expressed as absorbance percentage of the control. The data are expressed as the mean ± SE of 3 different experiments. *$P < 0.05$; **$P < 0.01$; ***$P < 0.001$

Colonosphere formation assay

Disaggregated PROM1/CD133+ cells were plated at 100 cells/well in a 24-well ultra-low attachment plate and treated with PDT (1.3 J/cm²) either in the presence and absence of CQ (10 µM), 3-MA (5 mM), sh*ATG3*, and sh*ATG5*. The number of the newly formed colonospheres/well was determined after 7 d. Colonospheres containing more than 20 cells were quantified for 8 different wells. The results are expressed as the mean ± SE of 3 different experiments.

Western blotting

Cell lysates were harvested from each cell subclone by resuspending the cells in 1× RIPA Lysis Buffer (Millipore, 20-188) at 24 h after PDT treatment (1.3 J/cm²). Equal amounts of protein extracts were resolved on SDS-PAGE gels and transferred to a PVDF membrane (Millipore, IPVH00010). Primary antibodies against the following molecules were used for the analysis: BECN1 (3495P), ATG3 (3415P), ATG5 (2630S), ATG7 (2631S), ATG12 (4180P) were purchased from Cell Signaling Technology. LC3B (GTX100240) and ACTB/β-ACTIN

(GTX110564) were obtained from GeneTex Inc. The specific reactive bands were detected using a goat anti-rabbit IgG antibody conjugated to horse radish peroxidase (GeneTex Inc., GTX213110-01). The immune complexes were visualized using the Western Lightning® Plus-ECL (PerkinElmer Inc., NEL104001EA), and quantification was performed using Image Quant software (GE Healthcare).

Lentivirus production and transduction

The shRNA-expression vectors, *ATG3* (TRCN0000147381) and *ATG5* (TRCN0000151474) shRNA constructs, were purchased from the National RNAi Core Facility (Taipei, Taiwan). For virus packaging, *psPAX2* (Addgene, Plasmid 12260), *pMD2.G* (Addgene, Plasmid 12259), and shRNA-expression vectors were cotransfected into 293T cells (form National RNAi Core Facility). The supernatant was harvested after 48 h. The viral supernatant fraction was filtered and used to infect PROM1/CD133+ cells in the presence of 8 μg/ml Polybrene® (Santa Cruz, sc-134220). Subsequently, these infected cells were selected by 2 μg/ml puromycin (InvivoGen, ant-pr-1). A *pGIPZ* lentiviral vector (Fisher Scientific, NC 9668406) was used as a negative control.

Apoptosis assay

Terminal deoxynucleotidyl transferase dUTP nick-end labeling (TUNEL) was performed according to the manufacturer's instructions of DeadEnd Fluorometric TUNEL system (Promega, G3250). Confocal imaging of apoptotic cells on slides was acquired using a LSM 5 confocal laser scanning microscope (Carl Zeiss MicroImaging, Jena, Germany) using LSM 5 Pascal software version 3.0. For excitation, a 488 nm argon laser was used for fluorescein-12-dUTP (emission collected with BP 520–555 nm filter), and the 405 nm diode laser was used for DAPI (emission collected with BP 415–480 nm filter).

The CASP3 activity assay was performed using the CaspACE™ Assay System, Colorimetric (Promega, G7220) according to the manufacturer's instructions. The results are presented as the mean CASP3 activity (± SE) of 3 different experiments.

Animal experiments

NOD/SCID mice were purchased from the National Laboratory Animal Center, Taiwan. All in vivo experimental procedures were approved by the National Taiwan University College of Medicine and College of Public Health Institutional Animal Care and Use Committee (IACUC). For xenograft tumor-seeding studies, PROM1/CD133+ PCCs pretreated with PDT (1.3 J/cm^2), CQ (10 μM), or sh*ATG5*, either alone or in the indicated combinations, were allowed to recover for 3 d in the absence of treatment. Then, 1×10^3 cells were injected subcutaneously into the flanks of NOD/SCID mice. Tumor incidence was observed for 12 wk after implantation. Tumor sizes were measured with calipers, and tumor volume was calculated as $(L * W^2)/2$ where L is the length and W is the width of the tumor.

Statistical analysis

All data from the WST-1 assays are expressed as the mean ± standard deviation. The *P* values were determined using an unpaired Student *t* test. *P* values < 0.05 were considered statistically significant.

Supplemental Materials

Supplemental materials may be found here:
www.landesbioscience.com/journals/autophagy/article/28679

References

1. Jemal A, Bray F, Center MM, Ferlay J, Ward E, Forman D. Global cancer statistics. CA Cancer J Clin 2011; 61:69-90; PMID:21296855; http://dx.doi.org/10.3322/caac.20107

2. Mulsow J, Merkel S, Agaimy A, Hohenberger W. Outcomes following surgery for colorectal cancer with synchronous peritoneal metastases. Br J Surg 2011; 98:1785-91; PMID:22034185; http://dx.doi.org/10.1002/bjs.7653

3. Wang JB, Liu LX. Use of photodynamic therapy in malignant lesions of stomach, bile duct, pancreas, colon and rectum. Hepatogastroenterology 2007; 54:718-24; PMID:17591048

4. Geltzer A, Turalba A, Vedula SS. Surgical implantation of steroids with antiangiogenic characteristics for treating neovascular age-related macular degeneration. Cochrane Database Syst Rev 2013; 1:CD005022; PMID:23440797

5. Moan J, Berg K. Photochemotherapy of cancer: experimental research. Photochem Photobiol 1992; 55:931-48; PMID:1409894; http://dx.doi.org/10.1111/j.1751-1097.1992.tb08541.x

6. Weishaupt KR, Gomer CJ, Dougherty TJ. Identification of singlet oxygen as the cytotoxic agent in photoinactivation of a murine tumor. Cancer Res 1976; 36:2326-9; PMID:1277137

7. Peng Q, Moan J, Nesland JM. Correlation of subcellular and intratumoral photosensitizer localization with ultrastructural features after photodynamic therapy. Ultrastruct Pathol 1996; 20:109-29; PMID:8882357; http://dx.doi.org/10.3109/01913129609016306

8. Piette J, Volanti C, Vantieghem A, Matroule JY, Habraken Y, Agostinis P. Cell death and growth arrest in response to photodynamic therapy with membrane-bound photosensitizers. Biochem Pharmacol 2003; 66:1651-9; PMID:14555246; http://dx.doi.org/10.1016/S0006-2952(03)00539-2

9. Gomer CJ, Ryter SW, Ferrario A, Rucker N, Wong S, Fisher AM. Photodynamic therapy-mediated oxidative stress can induce expression of heat shock proteins. Cancer Res 1996; 56:2355-60; PMID:8625311

10. Xue LY, Agarwal ML, Varnes ME. Elevation of GRP-78 and loss of HSP-70 following photodynamic treatment of V79 cells: sensitization by nigericin. Photochem Photobiol 1995; 62:135-43; PMID:7638257; http://dx.doi.org/10.1111/j.1751-1097.1995.tb05249.x

11. Robey RW, Steadman K, Polgar O, Bates SE. ABCG2-mediated transport of photosensitizers: potential impact on photodynamic therapy. Cancer Biol Ther 2005; 4:187-94; PMID:15684613; http://dx.doi.org/10.4161/cbt.4.2.1440

12. Gomer CJ, Luna M, Ferrario A, Rucker N. Increased transcription and translation of heme oxygenase in Chinese hamster fibroblasts following photodynamic stress or Photofrin II incubation. Photochem Photobiol 1991; 53:275-9; PMID:1826371; http://dx.doi.org/10.1111/j.1751-1097.1991.tb03934.x

13. Brackett CM, Owczarczak B, Ramsey K, Maier PG, Gollnick SO. IL-6 potentiates tumor resistance to photodynamic therapy (PDT). Lasers Surg Med 2011; 43:676-85; PMID:22057495

14. Jordan CT, Guzman ML, Noble M. Cancer stem cells. [Review]. N Engl J Med 2006; 355:1253-61; PMID:16990388; http://dx.doi.org/10.1056/NEJMra061808

15. Al-Hajj M, Becker MW, Wicha M, Weissman I, Clarke MF. Therapeutic implications of cancer stem cells. Curr Opin Genet Dev 2004; 14:43-7; PMID:15108804; http://dx.doi.org/10.1016/j.gde.2003.11.007

16. Ricci-Vitiani L, Lombardi DG, Pilozzi E, Biffoni M, Todaro M, Peschle C, De Maria R. Identification and expansion of human colon-cancer-initiating cells. Nature 2007; 445:111-5; PMID:17122771; http://dx.doi.org/10.1038/nature05384

17. Shmelkov SV, St Clair R, Lyden D, Rafii S. AC133/CD133/Prominin-1. Int J Biochem Cell Biol 2005; 37:715-9; PMID:15694831; http://dx.doi.org/10.1016/j.biocel.2004.08.010

18. Jin F, Zhao L, Zhao HY, Guo SG, Feng J, Jiang XB, Zhang SL, Wei YJ, Fu R, Zhao JS. Comparison between cells and cancer stem-like cells isolated from glioblastoma and astrocytoma on expression of anti-apoptotic and multidrug resistance-associated protein genes. Neuroscience 2008; 154:541-50; PMID:18462887; http://dx.doi.org/10.1016/j.neuroscience.2008.03.054

19. Dean M, Fojo T, Bates S. Tumour stem cells and drug resistance. Nat Rev Cancer 2005; 5:275-84; PMID:15803154; http://dx.doi.org/10.1038/nrc1590

20. Baumann M, Krause M, Hill R. Exploring the role of cancer stem cells in radioresistance. Nat Rev Cancer 2008; 8:545-54; PMID:18511937; http://dx.doi.org/10.1038/nrc2419

21. Rich JN. Cancer stem cells in radiation resistance. Cancer Res 2007; 67:8980-4; PMID:17908997; http://dx.doi.org/10.1158/0008-5472.CAN-07-0895

22. Morgan J, Jackson JD, Zheng X, Pandey SK, Pandey RK. Substrate affinity of photosensitizers derived from chlorophyll-a: the ABCG2 transporter affects the phototoxic response of side population stem cell-like cancer cells to photodynamic therapy. Mol Pharm 2010; 7:1789-804; PMID:20684544; http://dx.doi.org/10.1021/mp100154j

23. Klionsky DJ, Emr SD. Autophagy as a regulated pathway of cellular degradation. Science 2000; 290:1717-21; PMID:11099404; http://dx.doi.org/10.1126/science.290.5497.1717

24. Levine B. Eating oneself and uninvited guests: autophagy-related pathways in cellular defense. Cell 2005; 120:159-62; PMID:15680321

25. Eskelinen EL. New insights into the mechanisms of macroautophagy in mammalian cells. Int Rev Cell Mol Biol 2008; 266:207-47; PMID:18544495; http://dx.doi.org/10.1016/S1937-6448(07)66005-5

26. Codogno P, Meijer AJ. Autophagy and signaling: their role in cell survival and cell death. Cell Death Differ 2005; 12(Suppl 2):1509-18; PMID:16247498; http://dx.doi.org/10.1038/sj.cdd.4401751

27. White E, DiPaola RS. The double-edged sword of autophagy modulation in cancer. Clin Cancer Res 2009; 15:5308-16; PMID:19706824; http://dx.doi.org/10.1158/1078-0432.CCR-07-5023

28. Kim EH, Sohn S, Kwon HJ, Kim SU, Kim MJ, Lee SJ, Choi KS. Sodium selenite induces superoxide-mediated mitochondrial damage and subsequent autophagic cell death in malignant glioma cells. Cancer Res 2007; 67:6314-24; PMID:17616690; http://dx.doi.org/10.1158/0008-5472.CAN-06-4217

29. Apel A, Herr I, Schwarz H, Rodemann HP, Mayer A. Blocked autophagy sensitizes resistant carcinoma cells to radiation therapy. Cancer Res 2008; 68:1485-94; PMID:18316613; http://dx.doi.org/10.1158/0008-5472.CAN-07-0562

30. Reiners JJ Jr., Agostinis P, Berg K, Oleinick NL, Kessel D. Assessing autophagy in the context of photodynamic therapy. Autophagy 2010; 6:7-18; PMID:19855190; http://dx.doi.org/10.4161/auto.6.1.10220

31. Shen S, Kepp O, Kroemer G. The end of autophagic cell death? Autophagy 2012; 8:1-3; PMID:22082964; http://dx.doi.org/10.4161/auto.8.1.16618

32. Carew JS, Kelly KR, Nawrocki ST. Autophagy as a target for cancer therapy: new developments. Cancer Manag Res 2012; 4:357-65; PMID:23091399

33. Guo XL, Li D, Sun K, Wang J, Liu Y, Song JR, Zhao QD, Zhang SS, Deng WJ, Zhao X, et al. Inhibition of autophagy enhances anticancer effects of bevacizumab in hepatocarcinoma. J Mol Med (Berl) 2013; 91:473-83; PMID:23052483; http://dx.doi.org/10.1007/s00109-012-0966-0

34. He W, Wang Q, Xu J, Xu X, Padilla MT, Ren G, Gou X, Lin Y. Attenuation of TNFSF10/TRAIL-induced apoptosis by an autophagic survival pathway involving TRAF2- and RIPK1/RIP1-mediated MAPK8/JNK activation. Autophagy 2012; 8:1811-21; PMID:23051914; http://dx.doi.org/10.4161/auto.22145

35. Ito H, Daido S, Kanzawa T, Kondo S, Kondo Y. Radiation-induced autophagy is associated with LC3 and its inhibition sensitizes malignant glioma cells. Int J Oncol 2005; 26:1401-10; PMID:15809734

36. Tseng HC, Liu WS, Tyan YS, Chiang HC, Kuo WH, Chou FP. Sensitizing effect of 3-methyladenine on radiation-induced cytotoxicity in radio-resistant HepG2 cells in vitro and in tumor xenografts. Chem Biol Interact 2011; 192:201-8; PMID:21453691; http://dx.doi.org/10.1016/j.cbi.2011.03.011

37. Katayama M, Kawaguchi T, Berger MS, Pieper RO. DNA damaging agent-induced autophagy produces a cytoprotective adenosine triphosphate surge in malignant glioma cells. Cell Death Differ 2007; 14:548-58; PMID:16946731; http://dx.doi.org/10.1038/sj.cdd.4402030

38. Li YY, Lam SK, Mak JC, Zheng CY, Ho JC. Erlotinib-induced autophagy in epidermal growth factor receptor mutated non-small cell lung cancer. Lung Cancer 2013; 81:354-61; PMID:23769318; http://dx.doi.org/10.1016/j.lungcan.2013.05.012

39. Pan X, Zhang X, Sun H, Zhang J, Yan M, Zhang H. Autophagy inhibition promotes 5-fluorouraci-induced apoptosis by stimulating ROS formation in human non-small cell lung cancer A549 cells. PLoS One 2013; 8:e56679; PMID:23441212; http://dx.doi.org/10.1371/journal.pone.0056679

40. Eimer S, Belaud-Rotureau MA, Airiau K, Jeanneteau M, Laharanne E, Véron N, Vital A, Loiseau H, Merlio JP, Belloc F. Autophagy inhibition cooperates with erlotinib to induce glioblastoma cell death. Cancer Biol Ther 2011; 11:1017-27; PMID:21508666; http://dx.doi.org/10.4161/cbt.11.12.15693

41. Coupienne I, Bontems S, Dewaele M, Rubio N, Habraken Y, Fulda S, Agostinis P, Piette J. NF-kappaB inhibition improves the sensitivity of human glioblastoma cells to 5-aminolevulinic acid-based photodynamic therapy. Biochem Pharmacol 2011; 81:606-16; PMID:21182827; http://dx.doi.org/10.1016/j.bcp.2010.12.015

42. Traganos F, Darzynkiewicz Z. Lysosomal proton pump activity: supravital cell staining with acridine orange differentiates leukocyte subpopulations. Methods Cell Biol 1994; 41:185-94; PMID:7532261; http://dx.doi.org/10.1016/S0091-679X(08)61717-3

43. Lomonaco SL, Finniss S, Xiang C, Decarvalho A, Umansky F, Kalkanis SN, Mikkelsen T, Brodie C. The induction of autophagy by gamma-radiation contributes to the radioresistance of glioma stem cells. Int J Cancer 2009; 125:717-22; PMID:19431142; http://dx.doi.org/10.1002/ijc.24402

44. Dalby KN, Tekedereli I, Lopez-Berestein G, Ozpolat B. Targeting the prodeath and prosurvival functions of autophagy as novel therapeutic strategies in cancer. Autophagy 2010; 6:322-9; PMID:20224296; http://dx.doi.org/10.4161/auto.6.3.11625

45. Oleinick NL, Evans HH. The photobiology of photodynamic therapy: cellular targets and mechanisms. Radiat Res 1998; 150(Suppl):S146-56; PMID:9806617; http://dx.doi.org/10.2307/3579816

46. Song LL, Miele L. Cancer stem cells--an old idea that's new again: implications for the diagnosis and treatment of breast cancer. Expert Opin Biol Ther 2007; 7:431-8; PMID:17373895; http://dx.doi.org/10.1517/14712598.7.4.431

47. Jendzelovský R, Mikes J, Koval' J, Soucek K, Procházková J, Kello M, Sacková V, Hofmanová J, Kozubík A, Fedorocko P. Drug efflux transporters, MRP1 and BCRP, affect the outcome of hypericin-mediated photodynamic therapy in HT-29 adenocarcinoma cells. Photochem Photobiol Sci 2009; 8:1716-23; PMID:20024169; http://dx.doi.org/10.1039/b9pp00086k

48. Henderson BW, Busch TM, Vaughan LA, Frawley NP, Babich D, Sosa TA, Zollo JD, Dee AS, Cooper MT, Bellnier DA, et al. Photofrin photodynamic therapy can significantly deplete or preserve oxygenation in human basal cell carcinomas during treatment, depending on fluence rate. Cancer Res 2000; 60:525-9; PMID:10676629

49. Chen Q, Huang Z, Chen H, Shapiro H, Beckers J, Hetzel FW. Improvement of tumor response by manipulation of tumor oxygenation during photodynamic therapy. Photochem Photobiol 2002; 76:197-203; PMID:12194217; http://dx.doi.org/10.1562/0031-8655(2002)076<0197:IOTRBM>2.0.CO;2

50. Gibson SB. A matter of balance between life and death: targeting reactive oxygen species (ROS)-induced autophagy for cancer therapy. Autophagy 2010; 6:835-7; PMID:20818163; http://dx.doi.org/10.4161/auto.6.7.13335

51. Gong C, Bauvy C, Tonelli G, Yue W, Deloménie C, Nicolas V, Zhu Y, Domergue V, Marin-Esteban V, Tharinger H, et al. Beclin 1 and autophagy are required for the tumorigenicity of breast cancer stem-like/progenitor cells. Oncogene 2013; 32:2261-72, 1-11; PMID:22733132; http://dx.doi.org/10.1038/onc.2012.252

52. Chen H, Luo Z, Dong L, Tan Y, Yang J, Feng G, Wu M, Li Z, Wang H. CD133/prominin-1-mediated autophagy and glucose uptake beneficial for hepatoma cell survival. PLoS One 2013; 8:e56878; PMID:23437259; http://dx.doi.org/10.1371/journal.pone.0056878

53. Wu S, Wang X, Chen J, Chen Y. Autophagy of cancer stem cells is involved with chemoresistance of colon cancer cells. Biochem Biophys Res Commun 2013; 434:898-903; PMID:23624503; http://dx.doi.org/10.1016/j.bbrc.2013.04.053

54. Sasnauskiene A, Kadziauskas J, Vezelyte N, Jonusiene V, Kirveliene V. Damage targeted to the mitochondrial interior induces autophagy, cell cycle arrest and, only at high doses, apoptosis. Autophagy 2009; 5:743-4; PMID:19571672; http://dx.doi.org/10.4161/auto.5.5.8701

55. Dewaele M, Martinet W, Rubio N, Verfaillie T, de Witte PA, Piette J, Agostinis P. Autophagy pathways activated in response to PDT contribute to cell resistance against ROS damage. J Cell Mol Med 2011; 15:1402-14; PMID:20626525; http://dx.doi.org/10.1111/j.1582-4934.2010.01118.x

56. Bauvy C, Gane P, Arico S, Codogno P, Ogier-Denis E. Autophagy delays sulindac sulfide-induced apoptosis in the human intestinal colon cancer cell line HT-29. Exp Cell Res 2001; 268:139-49; PMID:11478840; http://dx.doi.org/10.1006/excr.2001.5285

57. Boya P, González-Polo RA, Casares N, Perfettini JL, Dessen P, Larochette N, Métivier D, Meley D, Souquere S, Yoshimori T, et al. Inhibition of macroautophagy triggers apoptosis. Mol Cell Biol 2005; 25:1025-40; PMID:15657430; http://dx.doi.org/10.1128/MCB.25.3.1025-1040.2005

58. Shimizu S, Takehara T, Hikita H, Kodama T, Tsunematsu H, Miyagi T, Hosui A, Ishida H, Tatsumi T, Kanto T, et al. Inhibition of autophagy potentiates the antitumor effect of the multikinase inhibitor sorafenib in hepatocellular carcinoma. Int J Cancer 2012; 131:548-57; PMID:21858812; http://dx.doi.org/10.1002/ijc.26374

59. Song J, Guo X, Xie X, Zhao X, Li D, Deng W, Song Y, Shen F, Wu M, Wei L. Autophagy in hypoxia protects cancer cells against apoptosis induced by nutrient deprivation through a Beclin1-dependent way in hepatocellular carcinoma. J Cell Biochem 2011; 112:3406-20; PMID:21769915; http://dx.doi.org/10.1002/jcb.23274

60. Yue W, Hamaï A, Tonelli G, Bauvy C, Nicolas V, Tharinger H, Codogno P, Mehrpour M. Inhibition of the autophagic flux by salinomycin in breast cancer stem-like/progenitor cells interferes with their maintenance. Autophagy 2013; 9:714-29; PMID:23519090; http://dx.doi.org/10.4161/auto.23997

61. Tanida I, Tanida-Miyake E, Komatsu M, Ueno T, Kominami E. Human Apg3p/Aut1p homologue is an authentic E2 enzyme for multiple substrates, GATE-16, GABARAP, and MAP-LC3, and facilitates the conjugation of hApg12p to hApg5p. J Biol Chem 2002; 277:13739-44; PMID:11825910; http://dx.doi.org/10.1074/jbc.M200385200

62. Hanada T, Noda NN, Satomi Y, Ichimura Y, Fujioka Y, Takao T, Inagaki F, Ohsumi Y. The Atg12-Atg5 conjugate has a novel E3-like activity for protein lipidation in autophagy. J Biol Chem 2007; 282:37298-302; PMID:17986448; http://dx.doi.org/10.1074/jbc.C700195200

63. Oral O, Oz-Arslan D, Itah Z, Naghavi A, Deveci R, Karacali S, Gozuacik D. Cleavage of Atg3 protein by caspase-8 regulates autophagy during receptor-activated cell death. Apoptosis 2012; 17:810-20; PMID:22644571; http://dx.doi.org/10.1007/s10495-012-0735-0

64. Yousefi S, Perozzo R, Schmid I, Ziemiecki A, Schaffner T, Scapozza L, Brunner T, Simon HU. Calpain-mediated cleavage of Atg5 switches autophagy to apoptosis. Nat Cell Biol 2006; 8:1124-32; PMID:16998475; http://dx.doi.org/10.1038/ncb1482

65. Maiuri MC, Zalckvar E, Kimchi A, Kroemer G. Self-eating and self-killing: crosstalk between autophagy and apoptosis. Nat Rev Mol Cell Biol 2007; 8:741-52; PMID:17717517; http://dx.doi.org/10.1038/nrm2239

66. Pyo JO, Jang MH, Kwon YK, Lee HJ, Jun JI, Woo HN, Cho DH, Choi B, Lee H, Kim JH, et al. Essential roles of Atg5 and FADD in autophagic cell death: dissection of autophagic cell death into vacuole formation and cell death. J Biol Chem 2005; 280:20722-9; PMID:15778222; http://dx.doi.org/10.1074/jbc.M413934200

67. Gong C, Song E, Codogno P, Mehrpour M. The roles of BECN1 and autophagy in cancer are context dependent. Autophagy 2012; 8:1853-5; PMID:22960473; http://dx.doi.org/10.4161/auto.21996

68. Ponti D, Costa A, Zaffaroni N, Pratesi G, Petrangolini G, Coradini D, Pilotti S, Pierotti MA, Daidone MG. Isolation and *in vitro* propagation of tumorigenic breast cancer cells with stem/progenitor cell properties. Cancer Res 2005; 65:5506-11; PMID:15994920; http://dx.doi.org/10.1158/0008-5472.CAN-05-0626